




Article

Calcium Biogeochemical Cycle in a Typical Karst Forest: Evidence from Calcium Isotope Compositions

Guilin Han ^{1,*} , Anton Eisenhauer ², Jie Zeng ¹  and Man Liu ¹ 

¹ Institute of Earth Sciences, China University of Geosciences (Beijing), Beijing 100083, China; zengjie@cugb.edu.cn (J.Z.); lman@cugb.edu.cn (M.L.)

² GEOMAR Helmholtz-Zentrum für Ozeanforschung Kiel, Wischhofstr. 1-3, 24148 Kiel, Germany; aeisenhauer@ifm-geomar.de

* Correspondence: hanguilin@cugb.edu.cn; Tel.: +86-10-82-323-536

Abstract: In order to better constrain calcium cycling in natural soil and in soil used for agriculture, we present the $\delta^{44/40}\text{Ca}$ values measured in rainwater, groundwater, plants, soil, and bedrock samples from a representative karst forest in SW China. The $\delta^{44/40}\text{Ca}$ values are found to differ by $\approx 3.0\%$ in the karst forest ecosystem. The Ca isotope compositions and Ca contents of groundwater, rainwater, and bedrock suggest that the Ca of groundwater primarily originates from rainwater and bedrock. The $\delta^{44/40}\text{Ca}$ values of plants are lower than that of soils, indicating the preferential uptake of light Ca isotopes by plants. The distribution of $\delta^{44/40}\text{Ca}$ values in the soil profiles (increasing with soil depth) suggests that the recycling of crop-litter abundant with lighter Ca isotope has potential effects on soil Ca isotope composition. The soil Mg/Ca content ratio probably reflects the preferential plant uptake of Ca over Mg and the difference in soil maturity. Light Ca isotopes are more abundant in mature soils than nutrient-depleted soils. The relative abundance in the light Ca isotope (^{40}Ca) is in the following order: farmland > burnt grassland > forests > grassland > shrubland. Our results further indicate that biological fractionation in a soil–plant system is a vital factor for Ca–geochemical transformations in soil surface systems.

Keywords: calcium cycle; calcium stable isotope; forest ecosystem; karst; Southwest China



Citation: Han, G.; Eisenhauer, A.; Zeng, J.; Liu, M. Calcium Biogeochemical Cycle in a Typical Karst Forest: Evidence from Calcium Isotope Compositions. *Forests* **2021**, *12*, 666. <https://doi.org/10.3390/f12060666>

Academic Editors: Jordi Voltas, Juan Pedro Ferrio and Tatiana A. Shestakova

Received: 16 April 2021

Accepted: 22 May 2021

Published: 25 May 2021

Publisher's Note: MDPI stays neutral with regard to jurisdictional claims in published maps and institutional affiliations.



Copyright: © 2021 by the authors. Licensee MDPI, Basel, Switzerland. This article is an open access article distributed under the terms and conditions of the Creative Commons Attribution (CC BY) license (<https://creativecommons.org/licenses/by/4.0/>).

1. Introduction

As an essential nutrient for plants, calcium (Ca) in organics-rich forest ecosystems (including mineral soils) is generally absorbed via the finer feeder roots of trees [1]. In particular, a major threat to forest ecosystem health is linked to the loss of environmental Ca [2]; therefore, many studies have focused on Ca sources and sinks in soils, plants, and the atmosphere across forest ecosystems [3–6]. Previous work has reported the use of $^{87}\text{Sr}/^{86}\text{Sr}$ (radiogenic Sr isotopic systems) and elemental ratios of Ba/Sr and Ca/Sr as typical tools for exploring Ca sources in forest ecosystems [7–10], while the application of Ca isotopes has been relatively limited due to high-precision measurements being difficult to perform. Radiogenic strontium isotope ratios, commonly used for distinguishing the sources of alkaline earth elements [8,11–14] due to its similar behavior to Ca in plant uptake processes and in ionic radius ($r_{\text{Sr}}/r_{\text{Ca}} = 1.13$), are now more often applied in studies of the biogeochemical cycle in forest ecosystem [7,9,10,12,15]. Although Ca and Sr are both alkaline earth elements, previous studies have suggested that these two elements are different [16,17]. In addition, the ionic behaviors of Ca^{2+} and Sr^{2+} are different in the long-term development of a forest ecosystem [18–21].

In recent studies, Ca isotope fractionation has been used in marine carbonate studies [22–26] and stable Ca isotopes have been applied directly to determine the biogeochemical cycle of elements in different ecosystems on Earth [3,4,21,27–38]. The results highlight the complex effects of biologically mediated trace metal cycling in forest ecosystems [3,4,21,29,31,38–40].

Many studies have confirmed that large amounts of Ca are available in the processes that internally circulate organic matter, in vegetation, and in the soil of forest ecosystems [41]. The litter-decomposition rates determine the Ca mineralization rates in vegetation, which varies significantly among different plant species [42,43]. For example, previous studies indicated that the base cation (including Ca and Mg) demands of American basswood and sugar maple are relatively high [44], resulting in different element turnover rates. Currently, whether Ca and Mg vary significantly in the bottom soil and surface soil under different vegetation covers is still unclear. In the present study, the $\delta^{44/40}\text{Ca}$ isotope compositions and Mg/Ca ratios of different forest ecosystem samples (rainwater, groundwater, soil, vegetation, and rock) were determined to understand the biogeochemical cycle of elements in Maolan areas, a representative subtropical karst forest in southwest China. In parallel, Ca in different pools were determined directly to further explore cycling processes involving Ca in karst forests. The main objectives are (1) to identify whether the stable isotope of Ca can be used to obtain quantified information about Ca uptake by plants during their life span and (2) to determine whether the Ca isotope composition of vegetation and associated soils can be used to better constrain Ca budgets in forests.

2. Materials and Methods

2.1. Geological Setting

In order to explore Ca biogeochemistry in a karst soil–plant system, a representative karst forest (Maolan National Natural Reserve Park, MNNRP) located in the southeast region of Guizhou Province (China) with a cover area of $\approx 213 \text{ km}^2$ and an elevation of $\approx 500 \text{ m}$ (Figure 1) was selected. The terrain is high in the northwest and low in the southeast. Well known for its good vegetation and rich fauna, the study area has a hot and humid tropical monsoon climate with an annual mean air temperature of $15.3 \text{ }^\circ\text{C}$. The wet season lasts from April to October, while the dry season lasts from November to March. The annual precipitation is $\approx 1750 \text{ mm}$ [45]. MNNRP is primarily covered by an evergreen broad-leaved forest ($\approx 88\%$), with plants such as incense cedar and *Taxus chinensis*, that effectively reduces water loss and soil erosion. Moreover, MNNRP has a well-developed karst landform with jagged carbonate rock (shallow marine carbonate) as well as sporadic sandstones (Figure 1). Black calcareous soil (shallow layer) dominates the study region due to lithological control (poor soil-forming capacity). Bare rocks on the ground lead to surface discontinuity, depleted water-holding capacity of the soil, and Ca-rich soil (salt base). Nevertheless, forest vegetation plays a key role in improving soil quality in MNNRP and in shaping the normal landscape and zonal vegetation.

2.2. Sampling Procedure

The calcium isotopic compositions of rainwater, groundwater, soils, forest tree leaves, crop leaves, and bedrock samples were measured. As shown in Figure 1, four rainwater samples were collected at the R site from June to September in 2008. Nine groundwater samples from springs and wells ($\approx 5 \text{ m}$ depth) were collected using a pre-cleaned sampler and bottles in July 2007 within the MNNRP (more details on the groundwater sites can be found in Reference [46]). Fifteen soil samples were collected from five typical soil profiles at different depths in the summer of 2007 [47], including farmland (LBP; 0, 40, and 110 cm), burnt grassland (LBM; 0, 40, and 70 cm), shrubland (LBS; 0, 40, and 90 cm), virgin forests (LBF; 0, 40, and 120 cm), and grassland (LBG; 0, 40, and 110 cm). Forest tree leaves, including the three most representative tree leaves from *Nandina domestica*, *Folium Platycaryae*, and *Handliodendron bodinier*, were collected during the summer of 2007 near the virgin forest soil site (LBF). Two crop leaves from soybean and corn were also collected at the farmland soil site (LBP) in 2007. A typical bedrock (dolomite rock) sample was collected near the virgin forest soil site (LBF) in 2007. The fresh plant samples were cleaned via ultrapure water, freeze dried, then put into a crushing device immersed in liquid nitrogen, and smashed into powder ($<150 \text{ }\mu\text{m}$). All of the soil and bedrock samples

were air-dried at ambient conditions and ground to less than 150 μm . The soils of five land use types had different pH and SOC values [47]. The cation concentrations of rainwater and groundwater were derived from our previous work [46,48].

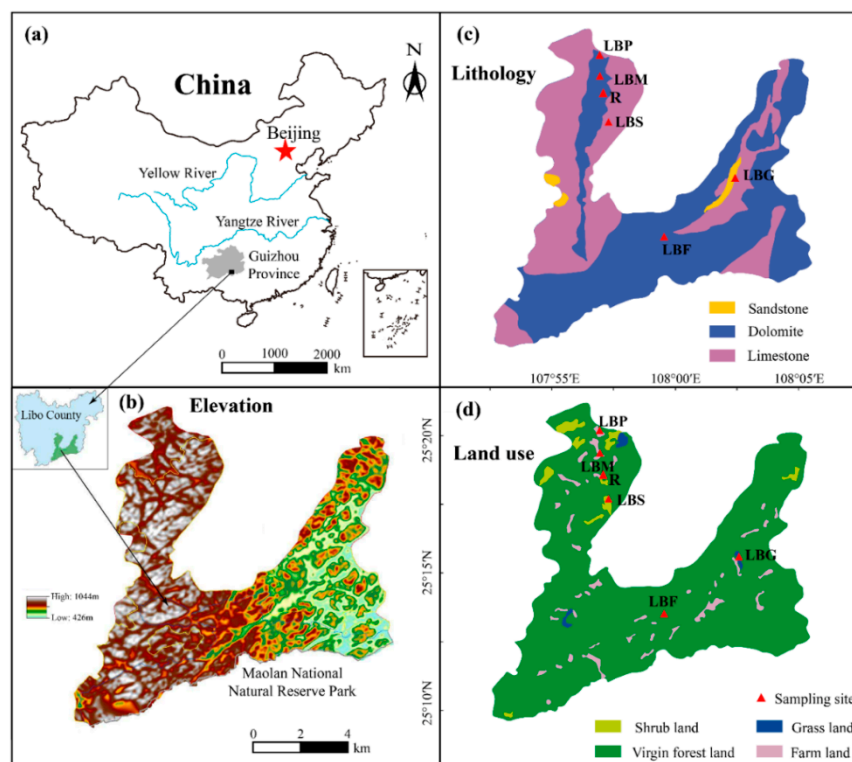


Figure 1. The study area and the soil sampling location: (a) location of MNNRP, (b) elevation of the study area, (c) lithology of the study area, and (d) land use of the study area. LBP, farmland soil site; LBM, burnt grassland soil site; LBS, shrubland soil site; LBF, virgin forest soil site; LBG, grassland soil site; R, rainwater site.

2.3. Chemical Analysis

For digestion of the plant, soil, and bedrock samples, (i) 100 mg of the sample powder was digested by 4 mL of 1:3 (*v/v*) HF and HNO_3 in a PFA sample jar (Savillex co., Eden Prairie, MN, USA) and then heated at 140 $^\circ\text{C}$ on a hotplate (≈ 7 d) to ensure complete digestion of the fluorides, carbon, and silicates [49–51]. The samples were dried subsequently. (ii) The dried samples were dissolved again in 4 mL of 1:3 (*v/v*) HF and HNO_3 using the same digestion procedure repeatedly until the solution became limpid. (iii) After complete digestion and drying, pure HNO_3 (2 mL) was applied two times to remove the fluorin and then vaporized using a hotplate. (iv) The remaining substance after digestion and after drying was dissolved in 100 mL volumetric flasks with 2% HNO_3 . All of the digestion processes were performed in an ultra-clean laboratory at the Institute of Geochemistry, Chinese Academy of Sciences (IGCAS). The concentrations of major cations were measured using ICP-OES in IGCAS. The measurement of a procedural blank, the standard reference material (GSB071192 and GSB071193), and sample replicates were performed during whole analyzation processes to ensure quality control. The accuracy of cations was better than $\pm 5\%$ for the quality control standards. The measurements of rainwater and groundwater samples were the same as those in our previous work [46,48].

2.4. Calcium Isotope Analysis

The double spike method was applied to measure Ca isotope compositions following the previous studies [30,52]. The ^{43}Ca and ^{48}Ca double spikes were added into all samples before the purification procedure. In the mixed solution of the sample and spike, the ^{40}Ca

and ^{44}Ca were all from the sample Ca while most of the ^{43}Ca and ^{48}Ca came from the spike Ca. Thus, according to the measured ratios for $^{40}\text{Ca}/^{48}\text{Ca}$, $^{44}\text{Ca}/^{48}\text{Ca}$, and $^{43}\text{Ca}/^{48}\text{Ca}$ (spike), all of the non-naturally derived Ca isotope fractionations during purification and measurements could be corrected. Calcium was separated from other elements on cation exchange resin columns (BioRad AGW 50x8 resin) using 1.5N HCl as an eluent, concluding a Ca blank of <2 ng (<0.7%) [52]. After drying, the mixed solution of the purified sample (about 300 ng Ca) and the spike were re-dissolved using 2.2 N HCl (1 μL). All of the purification procedures were conducted at GEOMAR [52]. For the thermal ionization mass spectrometer (TIMS) measurements of the Ca isotopes, the “sandwich technique (TaCl₅-activator solution)” and the out-gassed single filament (rhenium) were applied to preload the re-dissolved solution. Briefly, about 0.5 μL of TaCl₅-activator solution was first added onto the filament and heated to near dryness. Then, the re-dissolved sample (1 μL) was added on top of the activator solution and dried again. Another 0.5 μL of the activator solution was then added onto the filament and dried [52]. Finally, the Ca isotopes were measured via Triton T1 TIMS in GEOMAR following the method described in a previous work [52]. Two data-acquisition steps were performed in measurement processes since the cup configuration of Triton T1 TIMS does not cover the Ca mass range (40 to 48 amu) in a single step. In other words, the data for masses 40, 42, 43, and 44 were collected in the first step while that for 43 and 48 were detected simultaneously in the second step. Moreover, ^{41}K was also measured to evaluate the potential influence on mass ^{40}K isobaric interferences. The details for the double spike correction of the Ca isotope data can be found in a previous study [52]. Typically, the Triton T1 TIMS presented a ^{40}Ca signal intensity of 7–9 V during the measurement. The Ca isotope composition was expressed as $\delta^{44/40}\text{Ca} = [({}^{44}\text{Ca}/{}^{40}\text{Ca})_{\text{sample}} / ({}^{44}\text{Ca}/{}^{40}\text{Ca})_{\text{standard}} - 1] \times 1000$. NIST SRM 915a was applied as the standard reference material for the calculation of $\delta^{44/40}\text{Ca}$. The average value for repeat measurements was defined as the external precision (2SE). NIST SRM 915a presented a mean external precision of $\pm 0.09\text{‰}$ (2SD of the $\delta^{44/40}\text{Ca}$ values, reproducibility between runs, $n = 4$) and showed a mean $^{44}\text{Ca}/^{40}\text{Ca}$ value of 0.021182 ± 0.000006 (2σ , $n = 36$) during the entire measurement process.

3. Results

The Ca isotope compositions of the samples collected from MNNRP are summarized in Table 1 and Figure 2. The values measured from the forest ecosystem samples vary between -1.44‰ and 1.48‰ , corresponding to a $\approx 3.0\text{‰}$ natural variation in $\delta^{44/40}\text{Ca}$.

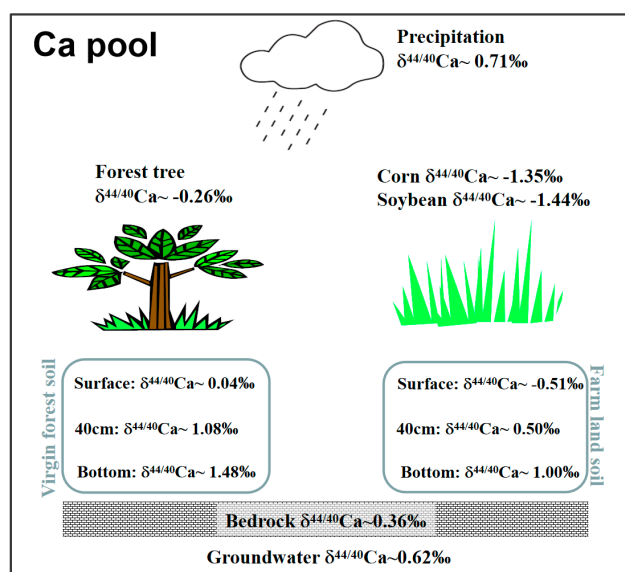


Figure 2. Ca isotope pool of the forest ecosystem in MNNRP.

Table 1. Ca and Mg concentrations and Ca isotopic composition of rainwater, groundwater, soil, vegetation, and bedrock samples in MNNRP.

Sample Number	Date (Year-Month-Day)	Ca ²⁺	Mg ²⁺	δ ^{44/40} Ca	2SD	n
		μmol/L	μmol/L	‰	‰	
Rainwater						
LB-32	2008-6-08	14.5	3.2	0.61	0.29	3
LB-41	2008-7-24	21.6	2.7	0.55	0.24	3
LB-44	2008-8-18	24.0	2.9	0.65	0.23	2
LB-47	2008-9-24	12.9	0.9	1.01	0.15	3
Groundwater						
2	2007-7-23	1163	648	0.40	0.14	2
3	2007-7-23	1309	501	0.52	0.04	3
7	2007-7-23	1312	373	0.60	-	1
11	2007-7-23	1452	114	0.63	-	1
13	2007-7-23	1728	289	0.72	-	1
16	2007-7-24	1759	126	0.36	0.13	2
20	2007-7-24	2538	394	0.43	0.01	2
24	2007-7-24	1334	1353	1.08	0.21	2
27	2007-7-27	1394	609	0.83	-	1
Bedrock		mmol/kg	mmol/kg			
Dolomite		6066	5872	0.36	0.09	3
Soil						
	depth (cm)					
Grassland	0	20	137	0.28	0.10	2
	40	56	135	0.75	0.14	3
	110	2275	2501	0.91	0.18	3
Shrubland	0	34	43	0.29	0.15	3
	40	159	166	0.30	0.24	3
	90	23	74	0.94	0.15	2
Farmland	0	106	464	-0.51	0.25	3
	40	13	16	0.50	0.22	3
	110	21	25	1.00	0.04	2
Burnt grassland	0	31	97	-0.38	0.19	2
	40	159	25	0.34	0.03	3
	70	16	25	1.00	0.15	2
Virgin forests	0	60	124	0.04	0.20	3
	40	11	36	1.08	0.21	2
	120	21	155	1.48	0.23	3
Forest tree						
<i>Nandian domestica</i>		231	101	-0.26	0.18	2
<i>Folium platycaryae</i>		602	194	-0.22	0.08	2
<i>Handliodendron bodinier</i>		672	234	-0.26	-	1
Crop						
Soybean		47	233	-1.44	0.14	3
Corn		51	249	-1.35	0.20	2

Note: the δ^{44/40}Ca values and uncertainties are based on two to three mass spectrometric measurements; the rainwater samples, groundwater samples, and soil samples were derived from our previous work [46–48]; 2SD, two times the standard deviation among the δ^{44/40}Ca values; n, number of measurements for each sample.

3.1. δ^{44/40}Ca Ratios of Rainwater

The δ^{44/40}Ca values of rainwater from the Maolan areas ranged from 0.55 ± 0.24‰ to 1.01 ± 0.15‰ (Figure 3), which is in agreement with the rainwater δ^{44/40}Ca variations observed in the United States [32], Europe [27], and Switzerland [36].

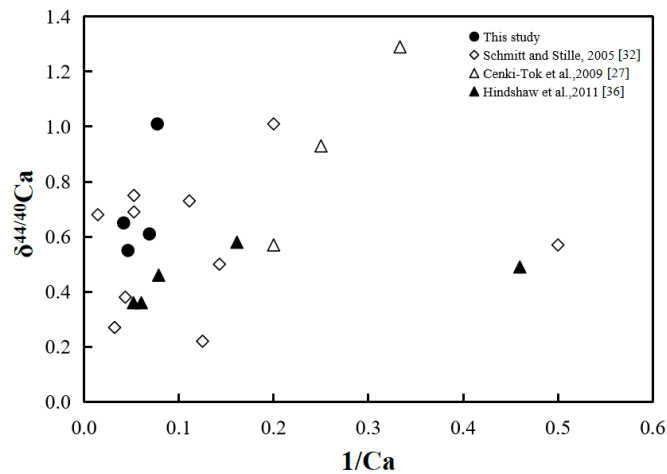


Figure 3. $\delta^{44/40}\text{Ca}$ (‰) vs. $1/\text{Ca}$ of rainwater samples in the MNNRP (this study) and other studies [27,32,36].

3.2. $\delta^{44/40}\text{Ca}$ Ratios of Groundwater

The $\delta^{44/40}\text{Ca}$ values of groundwater varied from $0.40 \pm 0.14\text{‰}$ to $1.08 \pm 0.21\text{‰}$ and are significantly heavier than the $\delta^{44/40}\text{Ca}$ values of dissolved Ca reported in rivers worldwide ($-1.71 \pm 0.23\text{‰}$ to $-0.63 \pm 0.07\text{‰}$) [16]. The $\delta^{44/40}\text{Ca}$ values of groundwater in MNNRP are also higher than those of the Yangtze River draining into carbonate-dominated catchments ($-0.63 \pm 0.07\text{‰}$) [26]. This interval overlaps with the $\delta^{44/40}\text{Ca}$ value of bedrock ($0.36 \pm 0.09\text{‰}$) and rainwater ($0.55 \pm 0.24\text{‰}$ to $1.01 \pm 0.15\text{‰}$).

3.3. $\delta^{44/40}\text{Ca}$ Ratios of Bedrock and Soils

The carbonate bedrock sample yielded a $\delta^{44/40}\text{Ca}$ value of $0.36 \pm 0.09\text{‰}$ (Table 1). The Ca concentrations of the surface soil pools in different soil profiles varied from 20 to 106 mmol/kg. Among the soil profiles, only the Ca concentration of grasslands increased with depth and relatively high Ca concentrations were found in the surface soil of farmland and virgin forests, while no obvious patterns were observed in the other profiles (Table 1). As shown in Figure 4, the $\delta^{44/40}\text{Ca}$ values of surface soil varied from $-0.51 \pm 0.25\text{‰}$ to $0.29 \pm 0.15\text{‰}$, lower than that of rainwater, groundwater, and bedrock. However, the pools of Ca in bottom soil varied from $0.91 \pm 0.18\text{‰}$ to $1.48 \pm 0.21\text{‰}$, higher than that of bedrock and surface soils. The $\delta^{44/40}\text{Ca}$ values of soil increased with depth in the soil profiles but were different for each soil profile. Simultaneously, it can be seen that the $\delta^{44/40}\text{Ca}$ values of surface farmland is the lowest (Figure 5), indicating the depletion of heavier isotopes in surface farmland relative to other soils. In contrast, grassland and shrubland show the highest $\delta^{44/40}\text{Ca}$ values, demonstrating ^{44}Ca enrichment compared with the virgin forests.

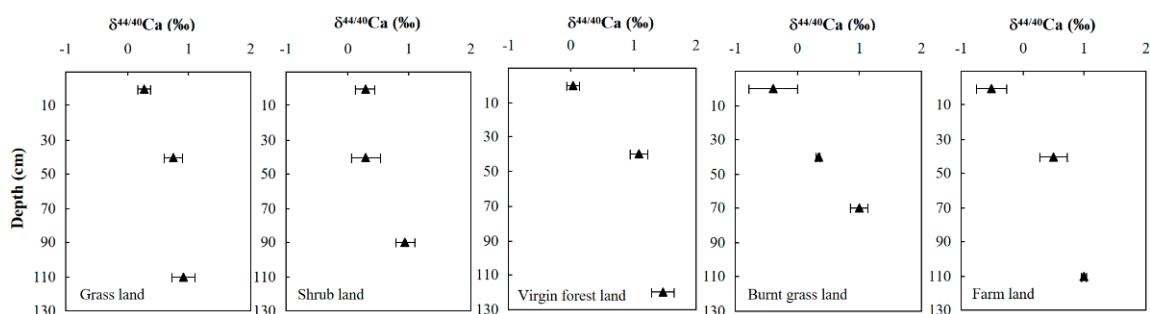


Figure 4. The $\delta^{44/40}\text{Ca}$ (‰) values from soil samples collected at different depths. Error bars are 2SD.

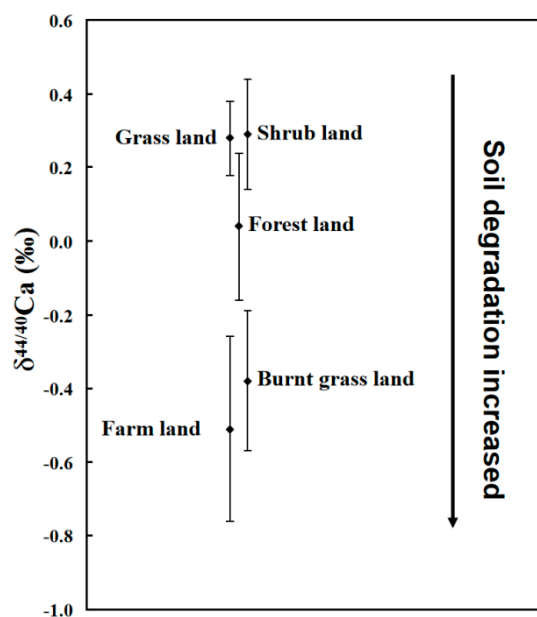


Figure 5. The $\delta^{44/40}\text{Ca}$ of surface soil under different vegetation covers in MNNRP. Error bars are 2SD.

3.4. $\delta^{44/40}\text{Ca}$ Ratios of Vegetation

Vegetation yields the lowest $\delta^{44/40}\text{Ca}$ values and the highest Ca concentrations in the forest ecosystem (Table 1). *Nandian domestica*, a typical shrub in Maolan, generates leaves characterized by a $\delta^{44/40}\text{Ca}$ value of $-0.26 \pm 0.18\%$. *Folium platycaryae* and *Handliodendron bodinier* are two typical arbors widely distributed in Maolan with $\delta^{44/40}\text{Ca}$ values of $-0.22 \pm 0.08\%$ and $-0.26 \pm 0.00\%$ in their leaves, respectively. All of the $\delta^{44/40}\text{Ca}$ values from the three natural leaf samples are similar.

Crops yield the lowest $\delta^{44/40}\text{Ca}$ values and relatively high Ca concentrations (Table 1) in comparison to other plants. Soybean is a typical crop in Maolan characterized by a $\delta^{44/40}\text{Ca}$ value of $-1.44 \pm 0.14\%$. The $\delta^{44/40}\text{Ca}$ value of Maize is $-1.35 \pm 0.20\%$.

4. Discussion

4.1. Atmospheric Inputs of Calcium

In general, two distinct sources are suggested to be the main contributors of Ca in groundwater: one is atmospheric input, and the other is bedrock weathering. Although the lowest Ca concentrations were observed in rainwater (12.9–24.0 $\mu\text{mol/L}$) and the Ca concentration in groundwater (1163–2538 $\mu\text{mol/L}$) is tens of times greater than that in rainwater, the range of $\delta^{44/40}\text{Ca}$ values in rainwater (0.55‰ to 1.01‰) is completely within the range of $\delta^{44/40}\text{Ca}$ values in groundwater (0.40‰ to 1.08‰) (Table 1). A previous study observed similar results in rainwater, snow, and throughfall samples in the Strengbach catchment [27]. Therefore, $\delta^{44/40}\text{Ca}$ values in groundwater reflect atmospheric input to a certain extent. Carbonate rocks generally have high Ca concentrations and relatively low $\delta^{44/40}\text{Ca}$ values [53–56]. In MNNRP, bedrock has the highest Ca concentration (6066 mmol/kg) and a $\delta^{44/40}\text{Ca}$ value (0.36‰) close to that for groundwater. Thus, both local carbonate rock weathering and atmospheric inputs tend to be responsible for (a potential source of) the Ca isotope compositions of groundwater in MNNRP, which also indicates that carbonate dissolution does not give rise to significant Ca isotopic fractionation. Our $^{87}\text{Sr}/^{86}\text{Sr}$ data also support this finding (more details will be published elsewhere).

4.2. Plant and Soil Calcium

Generally, Ca is absorbed by plants via fine lateral roots, then transported, and redistributed to different organs through the xylem sap. After autumn, mineralized Ca in

the litter of leaves and fruits is migrated to soil solutions, where it is partially reabsorbed by plants [41,57]. During pedogenesis, the contents of Ca and Mg in the soil decrease due to the combined influence of plant uptake (as important micronutrients for plants) and the rock weathering process (yielding elements/soluble components in the soil and further being potentially removed by groundwater [58,59]). The increasing Mg/Ca ratio shows a higher plant utilization rate for Ca than for Mg (or a potential higher groundwater-removal rate of Ca than for Mg), probably indicating soil maturation and that pedogenesis started. Considering the comparable effects of the weathering process and the subsequent groundwater-removal process on soil Ca and Mg contents in a local region, it is reasonably assumed that the longer the pedogenic time, the higher the Mg/Ca ratio in soils may become under the impact of plants. The $\delta^{44/40}\text{Ca}$ value of bottom virgin forests (120 cm) is as high as $\approx 1.48\%$, and the $\delta^{44/40}\text{Ca}$ value of soybean is as low as -1.44% (Table 1 and Figure 4). Therefore, the total range of $\delta^{44/40}\text{Ca}$ values in the Maolan karst forest ecosystem is about 3.0% . This observation is in line with the reported results. In other words, the Ca uptake by plant (as nutrient) is an important reason for Ca isotope fractionation on the Earth's surface [16,27,31,38]. The light Ca isotopes are favored by plant absorption and results in the enrichment of heavy Ca isotopes in soil pools. This can be demonstrated particularly from the soybean ($\delta^{44/40}\text{Ca} = -1.44\%$) and corn ($\delta^{44/40}\text{Ca} = -1.35\%$) samples, which are both related to farmland (surface soil $\delta^{44/40}\text{Ca} = -0.51\%$). It also can be seen from Table 2 that $\delta^{44/40}\text{Ca}$ values of surface soil tend to decrease with the increase in Mg/Ca ratios (reflecting the increase in extraction and usage of Ca from the soil), except for shrubland; the $\delta^{44/40}\text{Ca}$ values of surface soil was negatively correlated with the Mg/Ca ratios ($r = -0.89, p < 0.05$). The increment of vegetation coverage and soil maturation lead to elemental discrimination and isotope fractionation in soils.

Table 2. The $\delta^{44/40}\text{Ca}$ values and Mg/Ca ratios of surface soil in MNNRP.

	Shrubland	Virgin Forests	Grassland	Burnt Grassland	Farmland
Mg/Ca	1.27	2.08	2.45	3.15	4.37
$\delta^{44/40}\text{Ca}$	0.29	0.04	0.28	-0.38	-0.51

A previous study also suggested that the total amount and the available pools of C, N, and P are the highest for forests and are less for shrublands and grasslands in the study area [60]. Moreover, the increasing $\delta^{44/40}\text{Ca}$ values were observed to be accompanied by more soil development in a longer pedogenic process in Ohia tree-dominated Hawaiian rainforests [21]. Although the $\delta^{44/40}\text{Ca}$ values in five soil profiles varied to different degrees (Figure 4), our data imply that the soil $\delta^{44/40}\text{Ca}$ values always increased with depth in the soil profiles with different vegetation covers. Surface pristine grassland and shrubland show the highest soil $\delta^{44/40}\text{Ca}$ values, whereas surface farmland shows the lowest soil $\delta^{44/40}\text{Ca}$ value (Table 1 and Figure 4). The lowest soil $\delta^{44/40}\text{Ca}$ value observed in surface farmland may reflect the recycling of crop-litter-rich organic matter, which tends to be isotopically lighter than the underlying soil. This also reflects the result of the Ca nutrient demand in crops: the light Ca isotopes were preferentially extracted by the roots so that the soil was relatively enriched with heavy Ca isotopes. The biological fraction effects can be a reasonable explanation for the fractionation of Ca isotopes. This can also be supported by the results of a previous study which concluded that the isotope compositions of roots are dominated by the source variations and fractionation mechanisms, whereas the translocation mechanism is governed by fractionation processes [61]. Moreover, considering the different depths of plants roots, the $\delta^{44/40}\text{Ca}$ of net fractionation processes would be higher if the roots spread within high $\delta^{44/40}\text{Ca}$ value soil, which is an important direction of further research.

4.3. Local-Scale Ca Cycling Effects in Maolan Karst Forest Ecosystem

Our data confirm that the plant uptake of Ca (as nutrient) is an important source of Ca isotope fractionation on the Earth's surface [21,38,57]. Although we did not calculate the Ca budgets in the forest ecosystem, Ca–geochemical transformations occur in a surface system. The vegetation leaves are enriched with ^{40}Ca compared with soil: the light Ca isotopes are preferentially absorbed by plants, resulting in heavy Ca isotopes remaining in the soil. Soil mineral weathering-derived calcium presented a higher $\delta^{44/40}\text{Ca}$ value (0.91‰ to 1.48‰) than bedrock (0.36‰). Therefore, mineral weathering cannot explain the heavy $\delta^{44/40}\text{Ca}$ compositions of soil pools.

The Maolan forest catchment may only be representative of a typical karst ecosystem, but the significant vegetation-related biological uptake of Ca flux is observed. Therefore, its consideration in the future is necessary. As a function of ambient variations with time, the processes of Ca isotopic enrichment in different environmental systems (e.g., different plant–soil systems) is of great significance in correcting the Ca biogeochemical cycle model [57].

5. Conclusions

We observed that rainwater and groundwater are more enriched with heavy ^{44}Ca than bedrock and that soils and plants are more abundant in light ^{40}Ca . The greater abundance of ^{40}Ca in nutrient-rich soils than in nutrient-depleted soils reflects the decomposition and recycling of plant litter. The sequence of abundance in ^{40}Ca is as follows: farmland > burnt grassland > forests > grassland > shrubland. The evolution of Ca isotopes in karst forest ecosystems implies that intensely weathered soils have increased $\delta^{44/40}\text{Ca}$ values and that the internal circulation of a nutrient pool controls the Ca cycle of forest ecosystems. The Ca isotope compositions of plants might record the fractionation produced via the dynamic equilibrium between soils and plants. Moreover, the soil Mg/Ca content ratio and the Ca isotope compositions probably reflect the preferential plants uptake of Ca over Mg and the different soil maturities. This study highlights that Ca isotopes may be useful in exploring (or quantifying in the future) the origins and sinks of Ca in forest ecosystems.

Author Contributions: Conceptualization, G.H.; data curation, G.H.; formal analysis, G.H.; funding acquisition, G.H.; investigation, G.H.; methodology, G.H. and A.E.; project administration, G.H.; resources, G.H.; software, G.H. and M.L.; supervision, G.H.; validation, G.H.; visualization, G.H.; writing—original draft, G.H., J.Z. and M.L.; writing—review and editing, G.H. and J.Z. All authors have read and agreed to the published version of the manuscript.

Funding: This research was funded jointly by National Natural Science Foundation of China, grant numbers 41661144029 and 41325010.

Data Availability Statement: The data presented in this study are available in Table 1.

Acknowledgments: The authors gratefully acknowledge Ana Kolevica and Florian Böhm for laboratory assistance and technical support. We also thank Qiu Tan and Yang Tang for sampling assistance and thank Shitong Zhang for the English polishing.

Conflicts of Interest: The authors declare no conflict of interests.

References

1. Momoshima, N.; Bondietti, E.A. Cation binding in wood: Applications to understanding historical changes in divalent cation availability to red spruce. *Can. J. For. Res.* **1990**, *20*, 1840–1849. [[CrossRef](#)]
2. Likens, G.E.; Driscoll, C.T.; Buso, D.C. Long-term effects of acid rain: Response and recovery of a forest ecosystem. *Science* **1996**, *272*, 244. [[CrossRef](#)]
3. Hindshaw, R.S.; Bourdon, B.; Pogge von Strandmann, P.A.E.; Vigier, N.; Burton, K.W. The stable calcium isotopic composition of rivers draining basaltic catchments in Iceland. *Earth Planet. Sci. Lett.* **2013**, *374*, 173–184. [[CrossRef](#)]
4. Hindshaw, R.S.; Reynolds, B.C.; Wiederhold, J.G.; Kiczka, M.; Kretzschmar, R.; Bourdon, B. Calcium isotope fractionation in alpine plants. *Biogeochemistry* **2013**, *112*, 373–388. [[CrossRef](#)]
5. Huntington, T.G. Assessment of calcium status in Maine forests: Review and future projection. *Can. J. For. Res.* **2005**, *35*, 1109–1121. [[CrossRef](#)]

6. Lawrence, A.D.; Bu, J.; Gokulakrishnan, P. The interactions between SO₂, NO_x, HCl and Ca in a bench-scale fluidized combustor. *J. Inst. Energy* **1999**, *72*, 34–40.
7. Blum, J.D.; Klaue, A.; Nezat, C.A.; Driscoll, C.T.; Johnson, C.E.; Siccama, T.G.; Eagar, C.; Fahey, T.J.; Likens, G.E. Mycorrhizal weathering of apatite as an important calcium source in base-poor forest ecosystems. *Nature* **2002**, *417*, 729–731. [[CrossRef](#)]
8. Bullen, T.D.; Bailey, S.W. Identifying calcium sources at an acid deposition-impacted spruce forest: A strontium isotope, alkaline earth element multi-tracer approach. *Biogeochemistry* **2005**, *74*, 63–99. [[CrossRef](#)]
9. Kennedy, M.J.; Hedin, L.O.; Derry, L.A. Decoupling of unpolluted temperate forests from rock nutrient sources revealed by natural ⁸⁷Sr/⁸⁶Sr and ⁸⁴Sr tracer addition. *Proc. Natl. Acad. Sci. USA* **2002**, *99*, 9639. [[CrossRef](#)]
10. Miller, E.K.; Blum, J.D.; Friedland, A.J. Determination of soil exchangeable-cation loss and weathering rates using Sr isotopes. *Nature* **1993**, *362*, 438–441. [[CrossRef](#)]
11. Åberg, G.; Jacks, G.; Hamilton, P.J. Weathering rates and ⁸⁷Sr/⁸⁶Sr ratios: An isotopic approach. *J. Hydrol.* **1989**, *109*, 65–78. [[CrossRef](#)]
12. Bailey, S.W.; Hornbeck, J.W.; Driscoll, C.T.; Gaudette, H.E. Calcium inputs and transport in a base-poor forest ecosystem as interpreted by Sr isotopes. *Water Resour. Res.* **1996**, *32*, 707–719. [[CrossRef](#)]
13. Elias, R.W.; Hirao, Y.; Patterson, C.C. The circumvention of the natural biopurification of calcium along nutrient pathways by atmospheric inputs of industrial lead. *Geochim. Cosmochim. Acta* **1982**, *46*, 2561–2580. [[CrossRef](#)]
14. Poszwa, A.; Dambrine, E.; Pollier, B.; Atteia, O. A comparison between Ca and Sr cycling in forest ecosystems. *Plant Soil* **2000**, *225*, 299–310. [[CrossRef](#)]
15. Åberg, G.; Jacks, G.; Wickman, T.; Hamilton, P.J. Strontium isotopes in trees as an indicator for calcium availability. *Catena* **1990**, *17*, 1–11. [[CrossRef](#)]
16. Schmitt, A.-D.; Chabaux, F.; Stille, P. The calcium riverine and hydrothermal isotopic fluxes and the oceanic calcium mass balance. *Earth Planet. Sci. Lett.* **2003**, *213*, 503–518. [[CrossRef](#)]
17. Schmitt, A.-D.; Stille, P.; Vennemann, T. Variations of the ⁴⁴Ca/⁴⁰Ca ratio in seawater during the past 24 million years: Evidence from δ⁴⁴Ca and δ¹⁸O values of Miocene phosphates. *Geochim. Cosmochim. Acta* **2003**, *67*, 2607–2614. [[CrossRef](#)]
18. Capo, R.C.; Stewart, B.W.; Chadwick, O.A. Strontium isotopes as tracers of ecosystem processes: Theory and methods. *Geoderma* **1998**, *82*, 197–225. [[CrossRef](#)]
19. Pearce, C.R.; Parkinson, I.J.; Gaillardet, J.; Charlier, B.L.A.; Mokadem, F.; Burton, K.W. Reassessing the stable (δ⁸⁸/⁸⁶Sr) and radiogenic (⁸⁷Sr/⁸⁶Sr) strontium isotopic composition of marine inputs. *Geochim. Cosmochim. Acta* **2015**, *157*, 125–146. [[CrossRef](#)]
20. Pearce, C.R.; Parkinson, I.J.; Gaillardet, J.; Chetelat, B.; Burton, K.W. Characterising the stable (δ⁸⁸/⁸⁶Sr) and radiogenic (⁸⁷Sr/⁸⁶Sr) isotopic composition of strontium in rainwater. *Chem. Geol.* **2015**, *409*, 54–60. [[CrossRef](#)]
21. Wiegand, B.A.; Chadwick, O.A.; Vitousek, P.M.; Wooden, J.L. Ca cycling and isotopic fluxes in forested ecosystems in Hawaii. *Geophys. Res. Lett.* **2005**, *32*. [[CrossRef](#)]
22. Fantle, M.S.; DePaolo, D.J. Ca isotopes in carbonate sediment and pore fluid from ODP Site 807A: The Ca²⁺_(aq)–calcite equilibrium fractionation factor and calcite recrystallization rates in Pleistocene sediments. *Geochim. Cosmochim. Acta* **2007**, *71*, 2524–2546. [[CrossRef](#)]
23. Farkaš, J.; Buhl, D.; Blenkinsop, J.; Veizer, J. Evolution of the oceanic calcium cycle during the late Mesozoic: Evidence from δ⁴⁴/⁴⁰Ca of marine skeletal carbonates. *Earth Planet. Sci. Lett.* **2007**, *253*, 96–111. [[CrossRef](#)]
24. Nägler, T.F.; Eisenhauer, A.; Müller, A.; Hemleben, C.; Kramers, J. The δ⁴⁴Ca-temperature calibration on fossil and cultured *Globigerinoides sacculifer*: New tool for reconstruction of past sea surface temperatures. *Geochem. Geophys. Geosyst.* **2000**, *1*. [[CrossRef](#)]
25. Skulan, J.; DePaolo, D.J.; Owens, T.L. Biological control of calcium isotopic abundances in the global calcium cycle. *Geochim. Cosmochim. Acta* **1997**, *61*, 2505–2510. [[CrossRef](#)]
26. Zhu, P.; Macdougall, J.D. Calcium isotopes in the marine environment and the oceanic calcium cycle. *Geochim. Cosmochim. Acta* **1998**, *62*, 1691–1698. [[CrossRef](#)]
27. Cenko-Tok, B.; Chabaux, F.; Lemarchand, D.; Schmitt, A.D.; Pierret, M.C.; Viville, D.; Bagard, M.L.; Stille, P. The impact of water–rock interaction and vegetation on calcium isotope fractionation in soil- and stream waters of a small, forested catchment (the Strengbach case). *Geochim. Cosmochim. Acta* **2009**, *73*, 2215–2228. [[CrossRef](#)]
28. Cobert, F.; Schmitt, A.-D.; Bourgeade, P.; Labolle, F.; Badot, P.-M.; Chabaux, F.; Stille, P. Experimental identification of Ca isotopic fractionations in higher plants. *Geochim. Cosmochim. Acta* **2011**, *75*, 5467–5482. [[CrossRef](#)]
29. Farkaš, J.; Déjeant, A.; Novák, M.; Jacobsen, S.B. Calcium isotope constraints on the uptake and sources of Ca²⁺ in a base-poor forest: A new concept of combining stable (δ⁴⁴/⁴²Ca) and radiogenic (εCa) signals. *Geochim. Cosmochim. Acta* **2011**, *75*, 7031–7046. [[CrossRef](#)]
30. Han, G.; Song, Z.; Tang, Y.; Wu, Q.; Wang, Z. Ca and Sr isotope compositions of rainwater from Guiyang city, Southwest China: Implication for the sources of atmospheric aerosols and their seasonal variations. *Atmos. Environ.* **2019**, *214*, 116854. [[CrossRef](#)]
31. Page, B.D.; Bullen, T.D.; Mitchell, M.J. Influences of calcium availability and tree species on Ca isotope fractionation in soil and vegetation. *Biogeochemistry* **2008**, *88*, 1–13. [[CrossRef](#)]
32. Schmitt, A.-D.; Stille, P. The source of calcium in wet atmospheric deposits: Ca-Sr isotope evidence. *Geochim. Cosmochim. Acta* **2005**, *69*, 3463–3468. [[CrossRef](#)]

33. Turchyn, A.V.; DePaolo, D.J. Calcium isotope evidence for suppression of carbonate dissolution in carbonate-bearing organic-rich sediments. *Geochim. Cosmochim. Acta* **2011**, *75*, 7081–7098. [[CrossRef](#)]
34. Wiegand, B.A.; Schwendenmann, L. Determination of Sr and Ca sources in small tropical catchments (La Selva, Costa Rica)—A comparison of Sr and Ca isotopes. *J. Hydrol.* **2013**, *488*, 110–117. [[CrossRef](#)]
35. van der Heijden, G.; Dambrine, E.; Pollier, B.; Zeller, B.; Ranger, J.; Legout, A. Mg and Ca uptake by roots in relation to depth and allocation to aboveground tissues: Results from an isotopic labeling study in a beech forest on base-poor soil. *Biogeochemistry* **2015**, *122*, 375–393. [[CrossRef](#)]
36. Hindshaw, R.S.; Reynolds, B.C.; Wiederhold, J.G.; Kretzschmar, R.; Bourdon, B. Calcium isotopes in a proglacial weathering environment: Damma glacier, Switzerland. *Geochim. Cosmochim. Acta* **2011**, *75*, 106–118. [[CrossRef](#)]
37. Holmden, C.; Bélanger, N. Calcium isotope fractionation in a boreal forest ecosystem. *Geochim. Cosmochim. Acta* **2006**, *70*, A261. [[CrossRef](#)]
38. Holmden, C.; Bélanger, N. Ca isotope cycling in a forested ecosystem. *Geochim. Cosmochim. Acta* **2010**, *74*, 995–1015. [[CrossRef](#)]
39. Fantle, M.S.; Tipper, E.T. Calcium isotopes in the global biogeochemical Ca cycle: Implications for development of a Ca isotope proxy. *Earth Sci. Rev.* **2014**, *129*, 148–177. [[CrossRef](#)]
40. Zeng, J.; Han, G.; Wu, Q.; Tang, Y. Effects of agricultural alkaline substances on reducing the rainwater acidification: Insight from chemical compositions and calcium isotopes in a karst forests area. *Agric. Ecosyst. Environ.* **2020**, *290*, 106782. [[CrossRef](#)]
41. Likens, G.E.; Driscoll, C.T.; Buso, D.C.; Siccama, T.G.; Johnson, C.E.; Lovett, G.M.; Fahey, T.J.; Reiners, W.A.; Ryan, D.F.; Martin, C.W.; et al. The biogeochemistry of calcium at Hubbard Brook. *Biogeochemistry* **1998**, *41*, 89–173. [[CrossRef](#)]
42. Dijkstra, F.A. Calcium mineralization in the forest floor and surface soil beneath different tree species in the northeastern US. *For. Ecol. Manag.* **2003**, *175*, 185–194. [[CrossRef](#)]
43. Dijkstra, F.A.; Van Breemen, N.; Jongmans, A.G.; Davies, G.R.; Likens, G.E. Calcium weathering in forested soils and the effect of different tree species. *Biogeochemistry* **2003**, *62*, 253–275. [[CrossRef](#)]
44. Fujinuma, R.; Bockheim, J.; Balster, N. Base-cation cycling by individual tree species in old-growth forests of upper michigan, USA. *Biogeochemistry* **2005**, *74*, 357–376. [[CrossRef](#)]
45. Zeng, J.; Han, G. Rainwater chemistry reveals air pollution in a karst forest: Temporal variations, source apportionment, and implications for the forest. *Atmosphere* **2020**, *11*, 1315. [[CrossRef](#)]
46. Han, G.; Tang, Y.; Wu, Q. Hydrogeochemistry and dissolved inorganic carbon isotopic composition on karst groundwater in Maolan, southwest China. *Environ. Earth Sci.* **2010**, *60*, 893–899. [[CrossRef](#)]
47. Han, G.; Li, F.; Tang, Y. Variations in soil organic carbon contents and isotopic compositions under different land uses in a typical karst area in Southwest China. *Geochem. J.* **2015**, *49*, 63–71. [[CrossRef](#)]
48. Han, G.; Tang, Y.; Wu, Q.; Tan, Q. Chemical and strontium isotope characterization of rainwater in karst virgin forest, Southwest China. *Atmos. Environ.* **2010**, *44*, 174–181. [[CrossRef](#)]
49. Zeng, J.; Han, G.; Yang, K. Assessment and sources of heavy metals in suspended particulate matter in a tropical catchment, northeast Thailand. *J. Clean. Prod.* **2020**, *265*, 121898. [[CrossRef](#)]
50. Li, X.; Han, G. One-step chromatographic purification of K, Ca, and Sr from geological samples for high precision stable and radiogenic isotope analysis by MC-ICP-MS. *J. Anal. At. Spectrom.* **2021**, *36*, 676–684. [[CrossRef](#)]
51. Wang, J.; Wang, L.; Wang, Y.; Tsang, D.C.W.; Yang, X.; Beiyuan, J.; Yin, M.; Xiao, T.; Jiang, Y.; Lin, W.; et al. Emerging risks of toxic metal(loid)s in soil-vegetables influenced by steel-making activities and isotopic source apportionment. *Environ. Int.* **2021**, *146*, 106207. [[CrossRef](#)] [[PubMed](#)]
52. Heuser, A.; Eisenhauer, A.; Gussone, N.; Bock, B.; Hansen, B.T.; Nägler, T.F. Measurement of calcium isotopes ($\delta^{44}\text{Ca}$) using a multicollector TIMS technique. *Int. J. Mass Spectrom.* **2002**, *220*, 385–397. [[CrossRef](#)]
53. De La Rocha, C.L.; DePaolo, D.J. Isotopic evidence for variations in the marine calcium cycle over the Cenozoic. *Science* **2000**, *289*, 1176–1178. [[CrossRef](#)] [[PubMed](#)]
54. Zeng, J.; Han, G. Preliminary copper isotope study on particulate matter in Zhujiang River, southwest China: Application for source identification. *Ecotoxicol. Environ. Saf.* **2020**, *198*, 110663. [[CrossRef](#)]
55. Liu, M.; Han, G.; Zhang, Q. Effects of agricultural abandonment on soil aggregation, soil organic carbon storage and stabilization: Results from observation in a small karst catchment, Southwest China. *Agric. Ecosyst. Environ.* **2020**, *288*, 106719. [[CrossRef](#)]
56. Liu, M.; Han, G.; Li, X. Comparative analysis of soil nutrients under different land-use types in the Mun River basin of Northeast Thailand. *J. Soils Sediments* **2021**. [[CrossRef](#)]
57. Schmitt, A.-D.; Cobert, F.; Bourgeade, P.; Ertlen, D.; Labolle, F.; Gangloff, S.; Badot, P.-M.; Chabaux, F.; Stille, P. Calcium isotope fractionation during plant growth under a limited nutrient supply. *Geochim. Cosmochim. Acta* **2013**, *110*, 70–83. [[CrossRef](#)]
58. Liu, J.; Han, G. Tracing riverine particulate black carbon sources in Xijiang River basin: Insight from stable isotopic composition and Bayesian mixing model. *Water Res.* **2021**, *194*, 116932. [[CrossRef](#)]
59. Liu, J.; Han, G. Major ions and $\delta^{34}\text{S}_{\text{SO}_4}$ in Jiulongjiang River water: Investigating the relationships between natural chemical weathering and human perturbations. *Sci. Total. Environ.* **2020**, *724*, 138208. [[CrossRef](#)]

-
60. Hu, Z.-L.; Pan, G.-X.; Li, L.-Q.; Du, Y.-X.; Wang, X.-Z. Changes in pools and heterogeneity of soil organic carbon, nitrogen and phosphorus under different vegetation types in Karst mountainous area of central Guizhou Province, China. *Acta Ecol. Sin.* **2009**, *29*, 4187–4195. (In Chinese with English abstract)
 61. Schmitt, A.-D.; Gangloff, S.; Labolle, F.; Chabaux, F.; Stille, P. Calcium biogeochemical cycle at the beech tree-soil solution interface from the Strengbach CZO (NE France): Insights from stable Ca and radiogenic Sr isotopes. *Geochim. Cosmochim. Acta* **2017**, *213*, 91–109. [[CrossRef](#)]